

Production of High-Strength Al/Al₂O₃/WC Composite by Accumulative Roll Bonding

Morteza Shamanian, Mahyar Mohammadnezhad, and Jerzy Szpunar

(Submitted February 17, 2014; in revised form May 6, 2014; published online June 7, 2014)

In this study, Al/Al₂O₃/WC composites were fabricated via the accumulative roll bonding (ARB) process. Furthermore, the microstructure evolution, mechanical properties, and deformation texture of the composite samples were reported. The results illustrated that when the number of cycles was increased, the distribution of particles in the aluminum matrix improved, and the particles became finer. The microstructure of the fabricated composites after eight cycles of the ARB process showed an excellent distribution of reinforcement particles in the aluminum matrix. Elongated ultrafine grains were formed in the ARB-processed specimens of the Al/Al₂O₃/WC composite. It was observed that as the strain increased with the number of cycles, the tensile strength, microhardness, and elongation of produced composites increased as well. The results indicated that after ARB process, the overall texture intensity increases and a different-strong texture develops. The main textural component is the Rotated Cube component.

Keywords accumulative roll bonding, mechanical properties, metal matrix composite, microstructure, texture

1. Introduction

The increasing demand for better fuel economy, reduction of exhaust gas emission, and higher operating efficiency of cars and other vehicles is prompting intensive research on light-weight structural materials. Based on the high strength-to-weight ratio, aluminum alloys offer potential for weight reduction of various vehicles and have thus become increasingly attractive for use in automobile and aerospace industries, and also for bicycle frames, bridge railings, and various welded structures. The relatively low mechanical properties of these materials (considerably lower than those of steels), however, hinders their widespread application (Ref 1-4). To improve these properties, various composites material can be developed and used. Metal matrix composites (MMCs) based on aluminum alloys are characterized by properties superior to the corresponding aluminum alloys. They have increased specific strength and stiffness, improved mechanical properties at high temperature, lower thermal expansion, and better wear resistance (Ref 5-7). Processing of metals and alloys by severe plastic deformation (SPD) is a procedure used to produce submicron and nanostructured ultrafine-grained (UFG) MMC materials.

Accumulative roll bonding (ARB) is a major SPD process for manufacturing sheets of UFG materials; in this method a SPD process is used to produce UFG MMC (Ref 7-10). A

number of studies have investigated the microstructures and mechanical properties of multilayered composite produced by the ARB process such as Al/SiC (Ref 1), Al/Cu (Ref 5), Al/Al₂O₃ (Ref 6), Al/Ni (Ref 9), Al/B₄C (Ref 11), and Al/WC (Ref 12). However, interests in ARB are focused on the mechanisms of grain refinement and the effect of strain on microstructural and mechanical properties evolution. Furthermore, no systematic work has been performed to study the effects of Al₂O₃ and WC addition on properties of multilayered Al produced by ARB method. The motivation for the study of multi-layered Al/Al₂O₃/WC composites produced by ARB process was to improve the mechanical properties. It is worth mentioning that to the best of our knowledge, this work is the first of its kinds to study the multi-layered Al/Al₂O₃/WC composite by ARB. Microstructures, mechanical properties, and texture evolution of the hybrid composite samples were investigated, and results were discussed.

2. Experimental Procedure

As-received commercial purity aluminum sheets (specifications are given in Table 1) with the length of 200 mm, width of 50 mm, and thickness of 1 mm and Al₂O₃/WC particles (with an average size of 100 μm) were used as raw materials. To produce Al/3 vol% Al₂O₃/WC composites, 4.83 g Al₂O₃/WC particles were uniformly dispersed between the two strips by a brush. The ARB process was carried out with no lubrication, using a laboratory rolling mill, with a loading capacity of 20 tons with a specific amount of reduction equal to 50%. Then, the roll-bonded strips were cut in half, and the same procedure was repeated up to eight cycles at room temperature. To achieve well bonding between layers, the surfaces of the sheets were degreased by acetone and then wire-brushed. Samples for microscopy observations were cut along the rolling direction (RD)—transverse direction (TD) plane of the composites strips. Microstructural investigation was carried out using Hitachi SU6600 Scanning Electron Microscopy (SEM)

Morteza Shamanian, and Mahyar Mohammadnezhad, Department of Materials Engineering, Isfahan University of Technology, 84156-83111 Isfahan, Iran; and Jerzy Szpunar, Department of Mechanical Engineering, University of Saskatchewan, Saskatoon, SK S7N5A9, Canada. Contact e-mail: shamanian@cc.iut.ac.ir.

Table 1 Specifications of initial aluminum

Material	Tensile strength, MPa	Elongation, %	Hardness, HV
Al 1100	155	7.2	34

equipped with Energy Dispersive x-ray Spectroscopy (EDS) and EBSD. The sample preparation for EBSD studies was quite extensive. The diamond polished samples were subsequently polished with 50 nm colloidal silica slurry for 6 h using Vibro Met 2 Vibratory polisher. For obtaining orientation maps a voltage of 20 kV, working distance of 15 mm, and a step size of 50 nm were used. The HKL CHANNEL5 software was used to perform EBSD analysis and post-processing. In the maps presented in this paper, the green lines correspond to low-angle boundaries (LABs) with misorientation angles ranging from 2° to 15° and the red lines correspond to high-angle boundaries (HABs) with misorientation angles exceeding 15° . The tensile tests were conducted at ambient temperature on a Hounsfield H50KS testing machine at an initial strain rate of $1.67 \times 10^{-4} \text{ s}^{-1}$. The tensile test specimens were machined from the ARB-processed sheets oriented along the RD according to the ASTM E8M standard. The specimens were prepared so that the tensile direction was parallel to RD of the sheets. Vickers microhardness test was done using a Akashi apparatus under a load of 100 g and time of 10 s on the plane of the samples. Microhardness test was done on the all samples in more than seven randomly selected points and the average number was reported. For textures evolution samples were prepared by the standard metallographic procedures such as cutting, grinding, and mechanical polishing. Texture measurement was done using Bruker D8 Discover diffractometer with a VANTEC 2000 two-dimensional x-ray diffraction system (XRD2) using Cu $K\alpha$ radiation.

3. Results and Discussion

3.1 Microstructure Evaluation

3.1.1 SEM Analysis. Figure 1 illustrates the SEM micrograph of the microstructures of the composites produced by the ARB method in different cycles. In the composite-fabricated ARB cycle, it is clear that there are large particle free zones and agglomerated and clustered in the initial cycles because the agglomerative nature of particles due to their high cohesive energy leads to an increase in the total surface area and their tendency to clump together. Moreover, in this state due to the existence of big clusters in the produced composite, the bonding between reinforcement and matrix was weak and there was porosity between the particles (Fig. 1a and b).

Figure 1(c) and (d) shows that after the two cycles, both large particle free zones and number of agglomerated $\text{Al}_2\text{O}_3/\text{WC}$ particles become smaller. During the ARB process, the aluminum was plastically deformed, but since the reinforcement particles were brittle, they could respond to the stress only by fracturing. Hence, the clusters were broken up into particles and as a result, they were uniformly distributed in all parts of the aluminum matrix. Figure 1(e) and (f) illustrates that after the four and six cycles of ARB, respectively. It can be seen that both alumina layer and WC clusters and particles were broken up into smaller platelets, clusters, and particles to get uniformly

distributed throughout the aluminum matrix, but it cannot be showed that these microstructures are completely uniform. As the ARB process progressed forward and after the eight cycles (Fig. 1g), the clusters and the particle free zones almost disappeared. In other words, the microstructure of the MMC produced after eight cycles indicated a wholly uniform distribution of the $\text{Al}_2\text{O}_3/\text{WC}$ particles in the aluminum matrix (Ref 11-13).

3.1.2 EBSD Analysis. The typical image quality map (IQ map), grain boundary misorientation map (GB map), and orientation color map obtained on the RD-TD plane of the sample processed by eight ARB cycles are presented in Fig. 2. In the GB maps, HABs with the misorientation angle more than 15° are shown as red lines, while LABs having the misorientation angle of $2\text{--}15^\circ$ as green lines. The microstructures illustrate an ultrafine lamellar structure, and the microstructure contains two kinds of alignments of the grains. One type is near the powder particles, where the grains are convex around the particles, and the second type is in areas far from the powder particles, where their alignment is parallel to RD. The grains are very fine (until about 400 nm). Moreover, wide bands filled with many black regions in the composite samples are shown in Fig. 2(a) and (b), which they are the bonded interfaces and the regions including the composite particles. It is obvious that near the particles the density of LABs is relatively high (Fig. 2d).

3.2 Mechanical Properties

The mechanical properties of the ARB-processed $\text{Al}/\text{Al}_2\text{O}_3/\text{WC}$ composites after different cycles are shown in Fig. 3. Tensile strength of composites at different cycles had considerable difference in comparison with aluminum sheets. The $\text{Al}/\text{Al}_2\text{O}_3/\text{WC}$ composite showed remarkable increase in tensile strength with increasing ARB cycles. The maximum tensile strength reached 260 MPa at the eighth cycle. In addition, elongation of primary sheet was 7.2% and increased as ARB process preceded and reached an amount of 10% after the eight cycles. Microstructural evolution indicated that by increasing the number of cycles, the distribution of the reinforcement particles in the aluminum matrix changes to be more uniform, these results in increased strength and elongation because the uniformity of reinforcement particles has a major effect on the strength and elongation of MMC (Ref 11, 13). Moreover, bonding quality of the reinforcement/matrix is another factor that affects the final strength and elongation of MMC. By increasing the number of cycles, the bonding between the reinforcement particles and the matrix becomes stronger due to increased rolling pressure. Moreover, the presence of porosity in composites, especially the porosity surrounding the reinforcement particles, results in a lower tensile strength and elongation, which is why porosity has a major effect on mechanical properties of MMC. When the number of ARB cycles increases, the porosity of the samples due to good formability of the aluminum matrix and rolling pressure decreases, so tensile strength and elongation increase. In general, tensile strength and elongation values increased gradually by increasing of ARB cycles due to decreased porosities, increased uniformity of the particles, decreased size of the reinforcement particles, and improved adhesion between the matrix and the particles (Ref 10-14).

Figure 4 shows microhardness variations of composites layers at different cycles of ARB process. It illustrates that, as cycles increased, microhardness of composites layers increased.

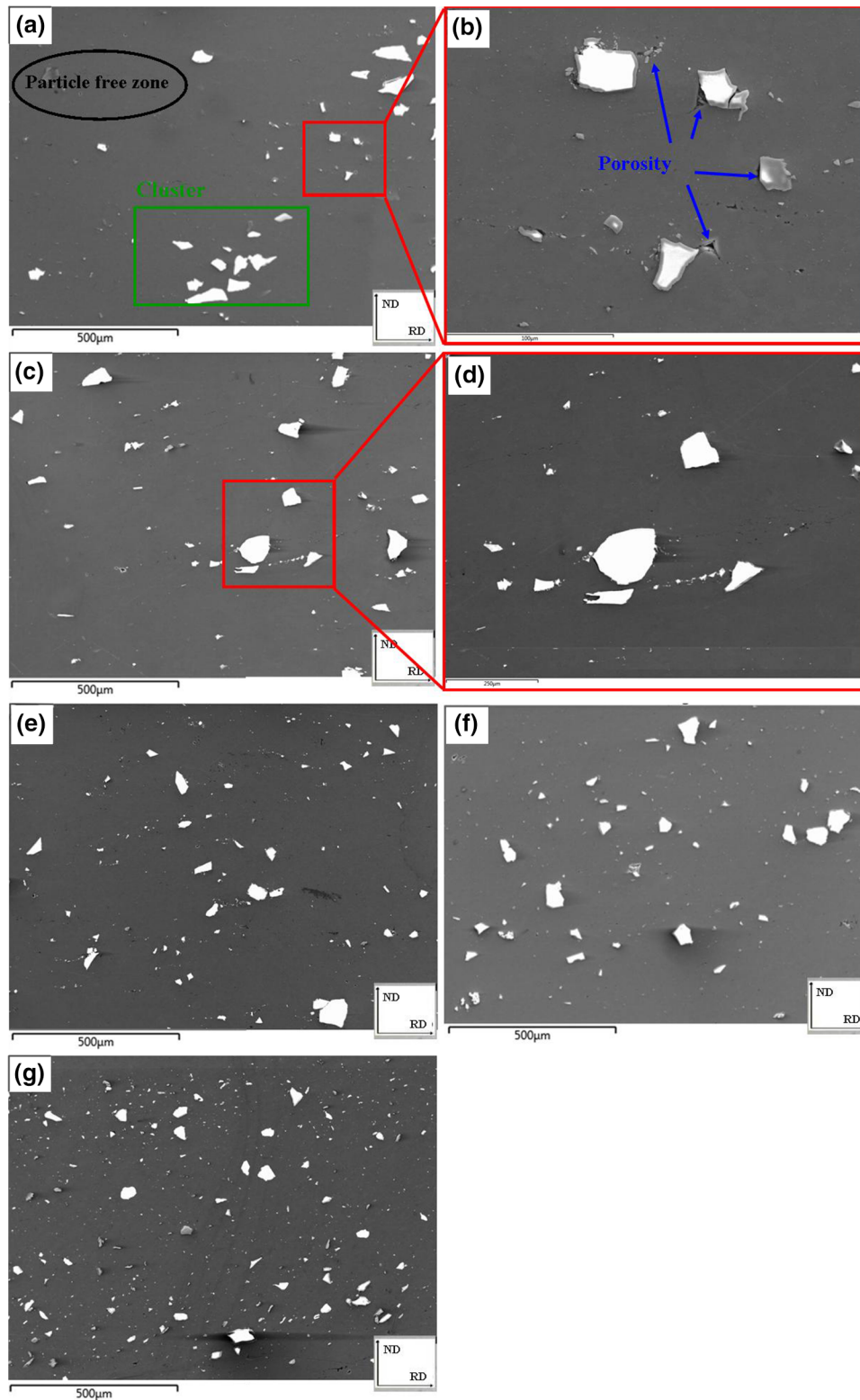


Fig. 1 Typical SEM microstructures of Al/Al₂O₃/WC composite after (a, b) one, (c, d) two, (e) four, (f) six, and (g) eight ARB cycles

The hardness of the as-received sheet was 34 HV, and after eight cycles ARB the hardness became 58 HV. It shows the largest increase in the early cycles of ARB, and then, a lower rate for the last cycles. Hardening behavior in ARB-processed ultrafine-grained structures follows a trend which reaches stable condition. Rapid increase in microhardness for rather low

strains was attributed mainly to the formation of subgrain boundaries and dislocations at the interface of composite layers, while grain refinement occurs in the later cycles. Previous results show that the grain refinement contributed less in the increase of microhardness than in the work hardening (Ref 2, 11-14).

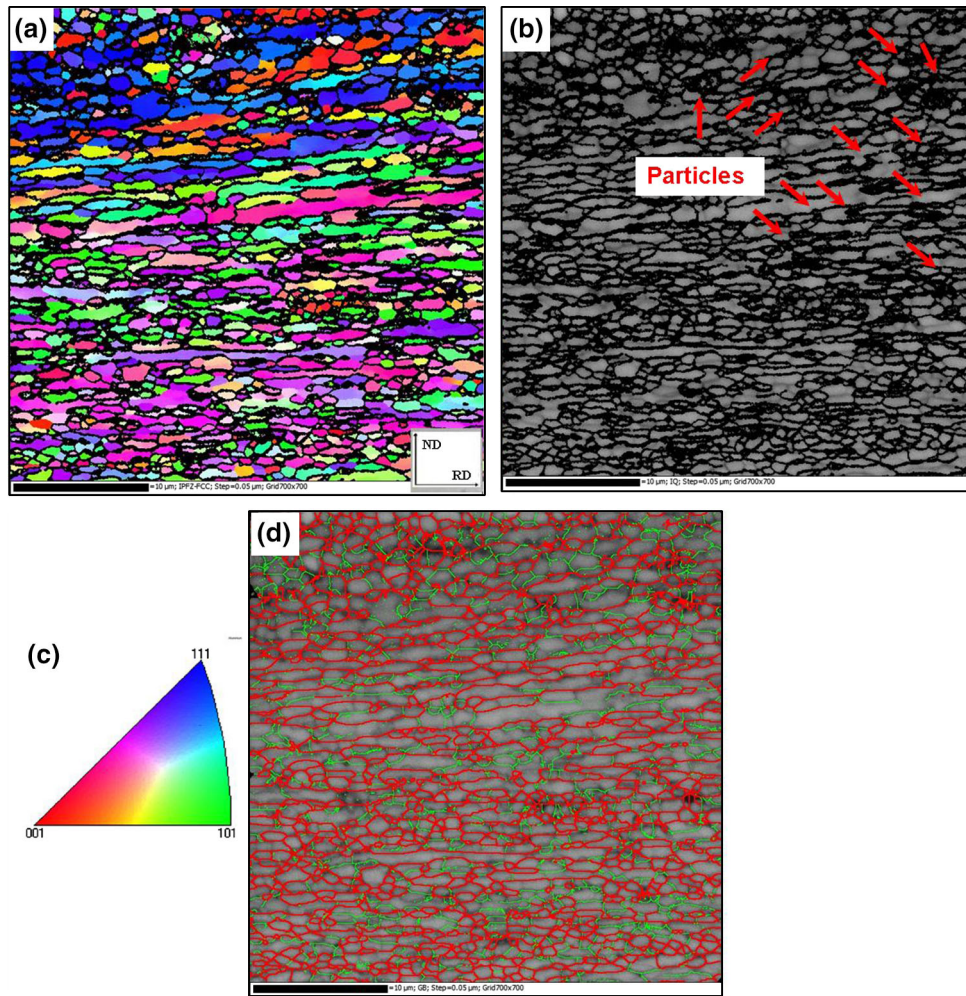


Fig. 2 EBSD maps of the Al/Al₂O₃/WC composite after eight cycles. (a) RD orientation color map (RD map). (b) IQ map. (c) Inverse pole figure (IPF) map. (d) Boundary misorientation map (GB) (Color figure online)

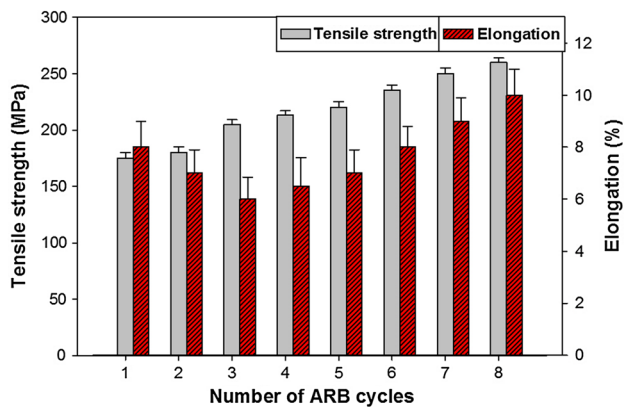


Fig. 3 The tensile strength and elongation variations of the composite produced by the ARB process vs. number of cycles

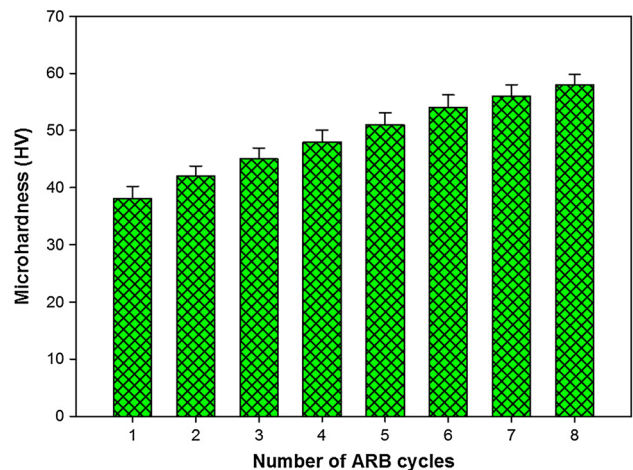


Fig. 4 Variation of microhardness after different rolling cycles

3.3 Texture Development

The (111) pole figures of the initial aluminum sheet and sample obtained on the surface RD-TD plane of the sample processed by eight ARB cycles are shown in Fig. 5. Figure 5(a) indicates that the main texture components are Cube, Goss,

Copper, and Dillamore with maximum intensity of $2.2 \times R$. Moreover, it can be seen that around each ideal component there is some scattering of intensity. In contrast to the as-received sheet, the pole figure after four and eight ARB cycles are obvious that

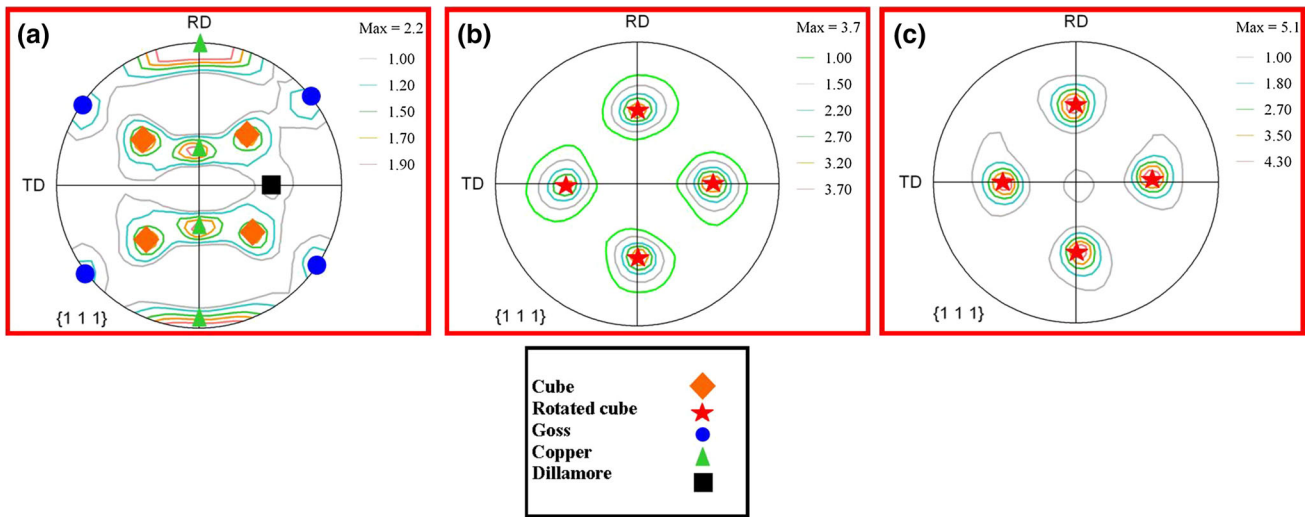


Fig. 5 {111} pole figures: (a) initial sheet, (b) after four ARB cycles, and (c) after eight ARB cycles

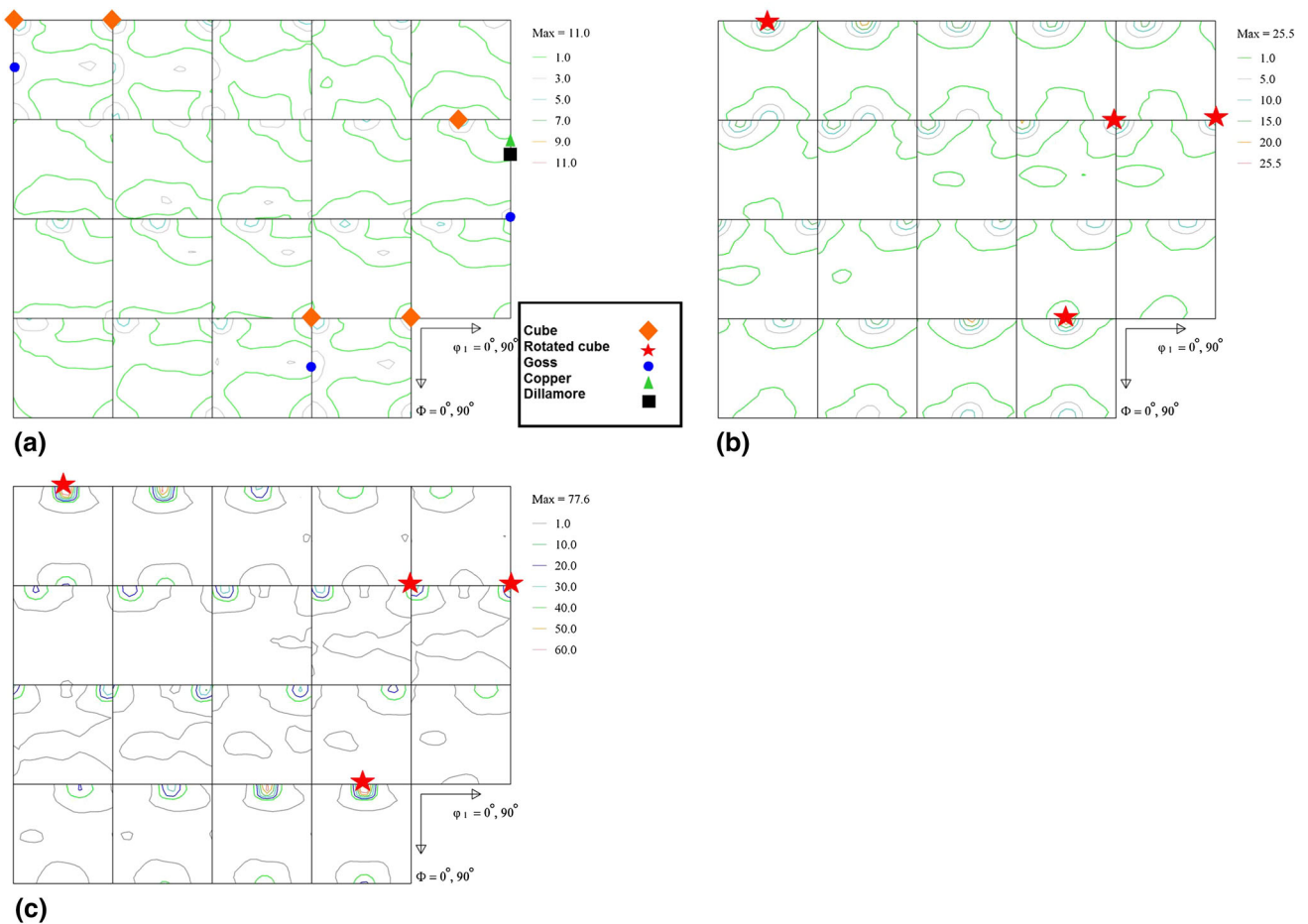


Fig. 6 ODFs: (a) initial sheet, (b) after four ARB cycles, and (c) after eight ARB cycles

the texture components are wholly different from that in the initial material. The maximum intensities after ARB were extremely increased compared to the previous sample and a new and sharp component was observed. The Rotated Cube component with a maximum intensity of 3.7 and $5.1 \times R$ for four and eight cycles,

respectively, is the single component. It can be seen that the textures in the sheet after ARB are very uniform and symmetry evident. The symmetry property is an important aspect to be considered in the quantitative analysis of textures and their correlations with deformation behavior during ARB process.

During ARB process, the grains might be getting subdivided by the formation of deformation bands due to the orientation splitting or microshear bands, so the subdivision of grains will lead to scatter around the ideal texture components and that is quite evident in the present case (Ref 15, 16).

The orientation distribution functions (ODFs) of initial sheet and both four and eight cycles ARBed composites are demonstrated in Fig. 6. A detailed analysis of textural evolution has been presented using ODFs because the ODF plots separate the components that partially overlap in the pole figures. Previous research indicated that there was no major change in the textural components as well as texture intensity in initial cycle ARB-processed composites, and texture evolution to saturate after many cycles (usually beyond four to eight) (Ref 16). Before ARB process, the Cube, Goss, Copper, and Dillamore make up major texture component. After various ARB cycles, the ODF shape changed and new components appeared. The important components which appeared after ARB process are Rotated Cube. In general, these samples show a transition texture that coincides with the corresponding pole figure. It must have, therefore, originated from recrystallization texture. After ARB, the intensities of the average texture are higher than that of the initial sheet. This shows that by ARB processing a very strong texture with sharp components develops. It has been reported that the evolution of this strong texture with very sharp component during the ARB leads to the formation of a band-like structure and prevents the full grain refinement to a submicron scale because the ARB-processed materials have quite complicated combinations of plane strain deformation and shear deformation (Ref 15-17). The ARB process depends on two parameters that the first parameter is the location of thickness. Thus, presence of Rotated Cube as the major texture component in this study can be slightly related to this parameter anyway. The number of cycles is the second parameter. The number of interfaces increases when the number of cycles is raised, so the distance between them decreases. By increasing the number of cycles due to increasing the interface number, and these interfaces have shear texture anyway, so the possibility of dominating the shear component becomes higher. Moreover, presence of Rotated Cube as the major texture component in this study is more attributed to this parameter. The presence of second phase particles can also change the texture evolution in the ARB processed. The presence of the second phase particles in the matrix results in large local lattice rotation and can cause different textures compared with the initial matrix. Thus, the overall texture intensity will be much sharper than the starting sheet. Kim et al. (Ref 18) reported that the second phase particles in the aluminum alloy sheets changed the texture intensity which is due to the inhomogeneous deformation around the second phase particles. A different texture caused by the presence of the reinforcement particles contributes to the transformation from low-angle subgrain boundaries to high-angle grain boundaries by increasing the misorientation between two adjacent subgrains and removes the unrefined bands from the microstructure (Ref 15-17).

4. Conclusions

The microstructure, mechanical properties, and deformation texture of the Al/Al₂O₃/WC composites produced by ARB

process were investigated. The following conclusions can be derived from experiments:

- By increasing the number of ARB cycles, the distribution of the reinforcement particles in the aluminum matrix increased and these particles became finer.
- The composites produced exhibited a higher tensile strength, elongation than the starting aluminum strips.
- The composites exhibited higher hardness due to work hardening and grain refinement.
- The texture evolution illustrated that the overall texture intensity increases and Rotated Cube was a major texture component after ARB process.

References

1. M. Alizadeh and M.H. Paydar, Fabrication of Nanostructure Al/SiCP Composite by Accumulative Roll-Bonding (ARB) Process, *J. Alloys Compd.*, 2010, **492**, p 231–235
2. A. Yazdani and E. Salahinejad, Evolution of Reinforcement Distribution in Al-B₄C Composites During Accumulative Roll Bonding, *Mater. Des.*, 2011, **32**, p 3137–3142
3. U.F.H.R. Suhuddin, S. Mironov, Y.S. Sato, and H. Kokawa, Grain Structure and Texture Evolution During Friction Stir Welding of Thin 6016 Aluminum Alloy Sheets, *Mater. Sci. Eng. A*, 2010, **527**, p 1962–1969
4. J. Khaled, A. Fadhlah, I. Abdulla, B. Almazrouee, and S. Abdulkareem, Microstructure and Mechanical Properties of Multi-pass Friction Stir Processed Aluminum Alloy 6063, *Mater. Des.*, 2014, **53**, p 550–560
5. M. Eizadjou, A. KazemiTalachi, H. DaneshManesh, H. ShakurShahabi, and K. Janghorban, Investigation of Structure and Mechanical Properties of Multi-layered Al/Cu Composite Produced by Accumulative Roll Bonding (ARB) Process, *Compos. Sci. Technol.*, 2008, **68**, p 2003–2009
6. R. Jamaati, M.R. Toroghinejad, M. Hoseini, and J. Szpunar, Texture Development in Al/Al₂O₃ MMCs Produced by Anodizing and ARB Processes, *Mater. Sci. Eng. A*, 2011, **528**, p 3573–3580
7. L. Ceschini, I. Boromei, G. Minak, A. Morri, and F. Tarterini, Effect of Friction Stir Welding on Microstructure, Tensile and Fatigue Properties of the AA7005/10 vol.% Al₂O₃p Composite, *Compos. Sci. Technol.*, 2007, **67**, p 606–615
8. A. Azushima, R. Kopp, A. Korhonen, D.Y. Yang, F. Micari, G.D. Lahoti, P. Groche, J. Yanagimoto, and N. Tsuji, Severe Plastic Deformation (SPD) Processes for Metals, *CIRP Ann*, 2008, **57**, p 716–735
9. A. Mozaffari, H. DaneshManesh, and K. Janghorban, Evaluation of Mechanical Properties and Structure of Multilayered Al/Ni Composites Produced by Accumulative Roll Bonding (ARB) Process, *J. Alloys Compd.*, 2010, **489**, p 103–109
10. N. Tsuji, Y. Ito, Y. Saito, and Y. Minamino, Strength and Ductility of Ultrafine Grained Aluminum and Iron Produced by ARB and Annealing, *Scr. Mater.*, 2002, **47**, p 893–899
11. M. Alizadeh, Comparison of Nanostructured Al/B₄C Composite Produced by ARB and Al/B₄C Composite Produced by ARB Process, *Mater. Sci. Eng. A*, 2010, **528**, p 578–582
12. C.Y. Liu, Q. Wang, Y.Z. Jia, B. Zhang, R. Jing, M.Z. Ma, Q. Jing, and R.P. Liu, Evaluation of Mechanical Properties of 1060-Al Reinforced with WC Particles via Warm Accumulative Roll Bonding Process, *Mater. Des.*, 2013, **43**, p 367–372
13. S. Amirhanlou, M.R. Rezaei, B. Niroumand, and M.R. Toroghinejad, High-Strength and Highly-Uniform Composites Produced by Compo-casting and Cold Rolling Processes, *Mater. Des.*, 2011, **32**, p 2085–2090
14. M. Eizadjou, H. DaneshManesh, and K. Janghorban, Mechanism of Warm and Cold Roll Bonding of Aluminum Alloy Strips, *Mater. Des.*, 2009, **30**, p 4156–4169

15. S. Pasebani and M.R. Toroghinejad, Nano-grained 70/30 Brass Strip Produced by Accumulative Roll-Bonding (ARB) Process, *Mater. Sci. Eng. A*, 2010, **527**, p 491–497
16. M. Raei, M.R. Toroghinejad, R. Jamaati, and J. Szpunar, Effect of ARB Process on Textural Evolution of AA1100 Aluminum Alloy, *Mater. Sci. Eng. A*, 2010, **527**, p 7068–7073
17. C. Liangwei, S. Qingnan, C. Dengquan, Z. Shiping, W. Junli, and L. Ximing, Research of Textures of Ultrafine Grains Pure Copper Produced by Accumulative Roll-Bonding, *Mater. Sci. Eng. A*, 2009, **508**, p 37–42
18. H.W. Kim, S.B. Kang, N. Tsuji, and Y. Minamino, Elongation Increase in Ultra-fine Grained Al-Fe-Si Alloy Sheets, *Acta Mater.*, 2005, **53**, p 1737–1749